Assessing the Evolutionary Nature of Multifragment Decay

E. Cornell, T. M. Hamilton, D. Fox,* Y. Lou, and R. T. de Souza
Department of Chemistry and Indiana University Cyclotron Facility, Indiana University, Bloomington, Indiana 47405

M. J. Huang, W. C. Hsi, C. Schwarz,† C. Williams, D. R. Bowman,* J. Dinius, C. K. Gelbke, T. Glasmacher, D. O. Handzy, M. A. Lisa,‡ W. G. Lynch, G. F. Peaslee,§ L. Phair,‡ and M. B. Tsang
National Superconducting Cyclotron Laboratory and Department of Physics and Astronomy, Michigan State University, East Lansing, Michigan 48824

G. VanBuren,‖ R. J. Charity, and L. G. Sobotka
Department of Chemistry, Washington University, St. Louis, Missouri 63130

W. A. Friedman
Department of Physics, University of Wisconsin, Madison, Wisconsin 53076
(Received 6 March 1995)

Multifragment decays of central collisions in $^{84}Kr + ^{197}Au$ at $E/A = 35$, 55, and 70 MeV are studied. The dependence of the extracted emission time on the velocity of the fragment pair is investigated. More energetic pairs manifest a stronger Coulomb interaction, indicating emission from a source of smaller spatial-temporal extent than less energetic pairs. This trend can be understood in the context of a statistical model that allows the source characteristics to evolve as the fragments are emitted.

PACS numbers: 25.70.Pq

Large, highly excited nuclear systems are observed to undergo the process of multifragmentation; i.e., they decay into a relatively large number of intermediate mass nuclear fragments (IMF's $3 \leq Z \leq 20$) [1–7]. Current evidence suggests that these fragments are produced from the decay of systems at low density [4,5]. Recent experimental results have been interpreted in terms of diametrically opposed scenarios regarding the importance of time in the fragmentation process [8–10]. Thus, a crucial open question regarding this process is whether IMF's are produced at a single time, from a well defined (freeze-out) condition, or whether they are produced over a period of time, as the system evolves and changes [11–13].

The inclusive kinetic energy spectra of fragments originating from central collisions provide no answer to this question. At a given angle these spectra are smooth, relatively featureless distributions that can be described by simple Boltzmann-like functions involving a single temperature, Coulomb barrier, and source velocity, and in some cases collective expansion energy. Typical spectra are shown in Fig. 1.

To explore the general systematics of multifragmentation, we have previously studied the dependence of fragment multiplicity on incident energy for the $^{84}Kr + ^{197}Au$ system in the range $E/A = 35$–400 MeV [14]. Light charged particles and IMF's produced in the collisions were detected in the angular range $5.4° \leq \theta_{lab} \leq 160°$ by the MSU Miniball/Washington University Miniwall 4π detector array. The energy resolution for this experiment was 15%. Experimental details have been previously described [14,15].

In this analysis, our attention is specifically directed to the question posed above, i.e., whether the fragments arise from a single condition, or during the evolution of the system. In order to preferentially select events from a single equilibrated source, we select on central collisions. We have related the charged particle multiplicity to an impact parameter scale following a geometrical prescription [16] and selected events that correspond to $b/b_{max} \leq 0.2$. In our definition, b_{max} refers to the maximum interaction radius for which two charged particles are emitted. These central collisions have charged particle multiplicities corresponding to $N_C \geq 24$, 33, and 38 at $E/A = 35$, 55, and

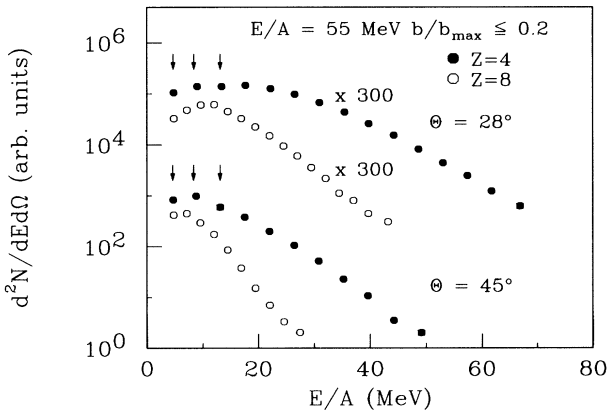

FIG. 1. Inclusive kinetic energy spectra for Be and O fragments (closed and open symbols) emitted in central collisions. The arrows indicate velocity cuts of $v_{min} = 3$, 4, and 5 cm/ns.

0031-9007/95/75(8)/1475(4)$06.00

70 MeV, respectively. For these central collisions the average multiplicity of IMF's, $\langle N_{\mathrm{IMF}} \rangle \approx 4$, 5, and 6 at $E/A = 35$, 55, and 70 MeV, respectively [14].

Our central question can be addressed by relating more exclusive observables to specific portions of the one-body energy spectrum. In particular, we examined the fragment-fragment velocity correlations for different portions of the one-body velocity distribution. If the multifragmentation process were to involve a sharp freeze-out, then one would expect little dependence of these fragment correlations on different portions of the energy spectrum. On the other hand, if the yield were to arise during the evolution of the system, then different components of the spectra may arise from different conditions, which could, in turn, provide different fragment-fragment correlation signals.

Fragment-fragment velocity correlations are a powerful tool for extracting information about the spatial-temporal dimensions of the emitting source [17–25]. This technique utilizes the mutual Coulomb repulsion of the fragments as a probe of the emitting system. The Coulomb repulsion results in a reduction of the probability for observing fragments at low relative velocity. Velocity correlation functions $R(v_{\mathrm{red}})$ were constructed, using procedures previously employed [20], by relating the coincidence yield Y_{12} to the product of the single particle yields Y_1 and Y_2:

$$\sum Y_{12}(v_1, v_2) = C[1 + R(v_{\mathrm{red}})] \sum Y_1(v_1) Y_2(v_2),$$

where v_1 and v_2 are the laboratory velocities of the fragments, the reduced velocity $v_{\mathrm{red}} = (v_1 - v_2)/(Z_1 + Z_2)^{1/2}$ [19], and C is a normalization constant determined by the requirement that $R(v_{\mathrm{red}}) \rightarrow 0$ at large relative velocities where the Coulomb repulsion is small. The single particle yields were constructed by selecting fragments from different events that satisfy the same constraints as the coincidence yield. The use of v_{red} allows summation over different charge combinations [19]. For the central collisions selected, the azimuthal distributions are relatively flat, indicating minimal distortions on the correlation function due to collective effects observed at higher incident energies [9].

As Figs. 2(a)–2(c) clearly indicate, the fragment-fragment correlation functions depend strongly on the kinetic energy of the fragment pairs. For each of the correlation functions shown, the fragments were selected on the basis of v_{min}, the minimum velocity of the less energetic fragment of each pair. All the correlation functions shown were summed over all pairs $4 \leq Z_1, Z_2 \leq 9$ emitted in the angular range $25° \leq \theta_{\mathrm{lab}} \leq 50°$. The normalization constant for each correlation function was determined in the range $0.05c \leq v_{\mathrm{red}} \leq 0.08c$. For orientation, the kinetic energies that correspond to these minimum velocities are depicted as the arrows on the energy spectra in Fig. 1. For the $E/A = 35$ MeV data the $v_{\mathrm{min}} = 5$ cm/ns correlation function was not shown because for this cut the correlation function at large v_{red} is not flat. This behavior could be due to dynamical effects (e.g., resonance decays, collective motion, etc.). All of the correlation functions exhibit a "Coulomb hole," a strong suppression of pairs of low relative velocity. As the minimum velocity of the pair is increased, a significant increase in the width of the Coulomb hole is observed at all three incident energies. To quantify this effect sufficiently to pursue qualitative observations,

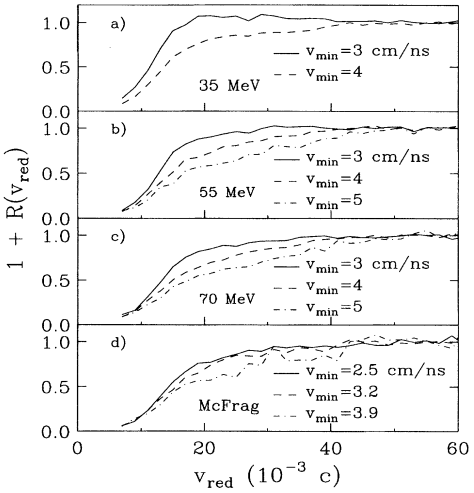

FIG. 2. (a)–(c) Experimental correlation functions at $E/A = 35$, 55, and 70 MeV with different restrictions on v_{min}. (d) Correlation functions constructed from the predictions of a microcanonical ensemble model for different restrictions on v_{min}.

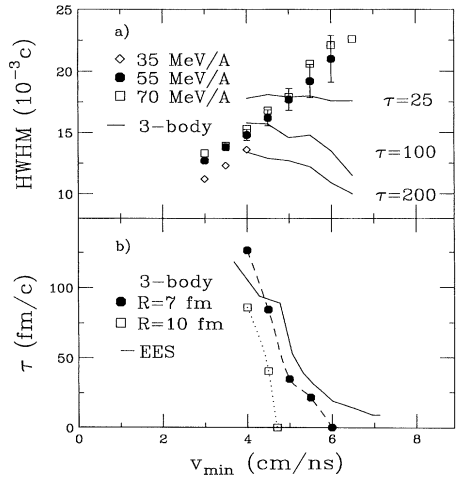

FIG. 3. (a) Dependence of the Coulomb interaction (HWHM) between fragments on the minimum fragment velocity. Diamonds, circles, and squares represent the experimental data at $E/A = 35$, 55, and 70 MeV. Solid lines indicate the results of three-body Coulomb trajectory calculations for $\tau = 25$, 100, and 200 fm/c. (b) Dependence of the extracted emission time on the minimum velocity of the fragment pair. The solid circles and open squares correspond to the experimental data at $E/A = 55$ MeV.

we have extracted the width of the Coulomb hole in the correlation function at half its asymptotic value (HWHM) for each cut of fragment energy. In Fig. 3(a), the values of the widths of the Coulomb holes are plotted against the velocity cutoff (minimum velocity) used to construct the correlation function. An increase in the HWHM with increasing v_{min} is clearly evident. For the v_{min} cuts shown, the correlation functions are affected by negligible dynamical effects. The representative error bars shown take into account the energy resolution. Selection of the same center-of-mass angle for each of the v_{min} cuts shown results in essentially the same trend observed in Fig. 3(a).

We next consider the possible implications of this trend. The shape of the correlation function is associated with the space-time structure of the fragment emission process. In general, the wider the Coulomb hole the smaller the separation in space-time between the emission of contributing fragment pairs. Thus, the dependence of the strength of the Coulomb interaction suggests that different space-time situations are associated with the emission related to different parts of the spectra. Specifically, the higher energy fragments are emitted with smaller space-time separation between fragments. This result is a clear indication of an evolutionary process.

In earlier studies of proton-proton correlations [26], similar investigations found that different effective source sizes for proton emission were associated with different proton momenta. This trend was interpreted as due to contributions to the one-body energy distribution from protons originating both from an early dynamical stage, as well as a late evaporative stage. This temporal behavior for proton emission is not surprising, however, since proton emission does not require attainment of a low density phase.

To further examine the general trends observed in the correlation functions, we have performed three-body Coulomb trajectory calculations in which we assume fragment emission from the surface of a source of fixed initial size. The source was assumed to be a nucleus with $Z = 40$, $A = 92$, and a radius of 7 fm [27]. The distribution function for the time between emissions was assumed to have the form $\exp(-t/\tau)$, which is characterized by a single characteristic time constant τ. Correlation functions, characterized by v_{min}, were constructed from the three-body Coulomb trajectory calculations. The observed inclusive correlation function, at 55 MeV/A, is well described by the decay of an $R = 7$ fm source with a characteristic emission time of $\tau = 100$ fm/c. Within the context of our three-body model, the dependence of the width of the Coulomb hole on the minimum velocity for different values of τ is shown as solid lines in Fig. 3(a).

While the reference three-body calculations for a given size and decay rate show a dependence of the predicted widths on velocity cutoff, the trend is opposite the trend observed in the data; namely, one finds a decrease in width with increasing minimum velocity. This decrease may simply be associated with an increase in the initial spatial separation of the members of the pair due to the increasing velocity of the first emitted fragment. If one were to assume that variation in time separation is more significant than the variation in spatial separation, and if one makes some reasonable assumption of source size, then each observed hole width can be associated with a given emission time constant through comparison with the three-body calculations. This procedure has been used to obtain the points displayed in Fig. 3(b), which relate mean emission times to the minimum velocity cutoffs in the spectra. The two different sets of points arise from the use of two different values for the source radius in the reference trajectory calculations.

We have examined the predicted relationship between emission rates and spectral velocities for two specific models of multifragmentation, the first, representative of the *freeze-out* scenario (where all fragments are formed at a single time), and the second, based on an *evolutionary* scenario (where the system changes as the fragments are emitted).

For the first model we have examined the Berlin microcanonical statistical model (McFrag) [28]. This model has previously been used to investigate the inclusive correlation function [29], but it fails to reproduce the fragment kinetic energy spectra, providing a very narrow range of fragment velocities. The source was assumed to have $Z = 79, A = 197$ with an excitation energy of 2400 MeV and a freeze-out radius of $\approx$13 fm. These parameters roughly reproduce the experimentally measured IMF and charged particle multiplicities at $E/A = 55$ MeV [23]. The dependence of the correlation function on the fragment velocity predicted by the McFrag model is shown in Fig. 2(d). The velocity cutoffs, differing from those in Figs. 2(a)–2(c), were scaled (based on the fraction of the velocity distribution) to the limited range of the spectra provided by the model. Since all the fragments are emitted simultaneously, the only dependence of the correlation function on final spectral velocity comes from the sampling of different initial spatial configurations of the final decay fragments. This feature appears to provide the correlation functions with only a weak dependence on the fragment kinetic energy.

For the second model we examined the predictions of the expanding emitting source (EES) model [13], which explicitly incorporates emission during the evolution of the system. While this model predicts smooth single fragment energy spectra, these spectra are composed of contributions arising from different times in the decay of the source. In this model, the source temperature changes with time due to adiabatic changes in density and particle emission. The Coulomb acceleration also changes with time. The portion of the spectra associated with each instant in time is provided by instantaneous properties. A schematic calculation was done for an initial source of $A = 197$ and $Z = 79$, with an initial temperature of 12 MeV. This calculation predicts an average multiplicity of about 4 IMF's. Because of the changing conditions, the mean separation

times vary with the velocity of the fragments. The calculation shows a decreasing mean emission (separation) time with increasing fragment energy. This result can be understood as follows: The most energetic part of the spectra is populated for the highest temperatures and Coulomb energies. These conditions exist only early in the evolution of the system. At later times, fragments of these kinetic energies are rarely emitted. This confined "window" of opportunity for high energy fragments affects the mean separation time associated with their emission. The model suggests that the mean separation time increases with decreasing fragment energy until the vicinity of the yield peak where it levels off. For the very lowest velocity fragments the separation times grows sharply. These fragments are predominately emitted under conditions of low temperature and low source charge, where the predicted emission process is slowest. An attempt has been made to compare the qualitative predictions of the EES model with the trends shown in Fig. 3(b). The model was used to predict the relationship between mean emission times and fragment velocities in the source frame for pairs of ^{9}Be fragments. The velocities of fragments predicted in the model were then transformed from the center-of-mass to the laboratory frame using the experimentally determined center-of-mass velocity. These transformed results have been compared with the experimental data in Fig. 3(b). The schematic model calculations do not reproduce the exact dependence of τ on $v_{\min}$, indicating that the precise relationship between changes in the source properties and fragment emission dynamics is not yet fully understood. The calculations do, however, predict a trend that is very similar to that observed experimentally, indicating that changes in the source characteristics and fragment formation occur on commensurate time scales.

In summary, we have examined the relationship between the fragment-fragment velocity correlation functions and the velocity of the fragments from which they are constructed, for central collisions in the reaction ^{84}Kr + ^{197}Au at E/A = 35, 55, and 70 MeV. In each of these cases there is an increase in the width of the Coulomb hole of the correlation function with increasing fragment velocity. This trend is opposite the trend obtained with trajectory calculations that assume a single decay constant and source size. The data appear inconsistent with a single freeze-out condition, and are not predicted by a model based on such a scenario. A statistical model that assumes fragment emission from an evolving system qualitatively predicts the general trend of the observed data. The strong relationship between the fragment velocities and the mean emission times suggests that there are changes in the character of the source on a time scale concurrent with the fragment emission, and thus that the mechanism of multifragmentation is evolutionary.

We would like to acknowledge the valuable assistance of the staff and operating personnel of the K1200 cyclotron at Michigan State University for providing the high quality beams which made this experiment possible. One of the authors (R. D.) gratefully acknowledges the support of the Sloan Foundation through the A. P. Sloan Fellowship program. W. A. F acknowledges the support of the National Institute for Nuclear Theory, University of Washington, Seattle. This work was supported by the U.S. Department of Energy under Contract No. DE-FG02-92ER40714 and the National Science Foundation under Grants No. PHY-89-13815, No. PHY-90-15957, No. PHY-93-14131, and No. PHY-92-14992.

*Present address: CRL, Chalk River, Ontario K0J 1J0, Canada.
†Present address: GSI, 94720, Darmstadt, Germany.
‡Present address: LBL, University of California, Berkeley, CA 94720.
§Present address: Department of Chemistry, Hope College, Holland, MI 49423.
‖Present address: Department of Physics, MIT, Cambridge, MA 02139.

[1] J. E. Finn *et al.*, Phys. Rev. Lett. **49**, 1321 (1982).
[2] J. W. Harris *et al.*, Nucl. Phys. **A471**, 241c (1987).
[3] C. A. Ogilvie *et al.*, Phys. Rev. Lett. **67**, 1214 (1991).
[4] R. T. de Souza *et al.*, Phys. Lett. B **268**, 6 (1991).
[5] D. R. Bowman *et al.*, Phys. Rev. Lett. **67**, 1527 (1991).
[6] G. Bertsch and P. J. Siemens, Phys. Lett. **126B**, 9 (1983).
[7] W. Bauer *et al.*, Phys. Rev. Lett. **58**, 863 (1987).
[8] M. L. Gilkes *et al.*, Phys. Rev. Lett. **73**, 1590 (1994).
[9] B. Kaempfer *et al.*, Phys. Rev. C **48**, R955 (1993).
[10] L. G. Moretto *et al.*, Phys. Rev. Lett. **74**, 1530 (1995).
[11] D. H. E. Gross *et al.*, Phys. Rev. Lett. **56**, 1544 (1986).
[12] J. Bondorf *et al.*, Nucl. Phys. **A444**, 460 (1985).
[13] W. A. Friedman, Phys. Rev. C **42**, 667 (1990).
[14] G. F. Peaslee *et al.*, Phys. Rev. C **49**, R2271 (1994).
[15] R. T. de Souza *et al.*, Nucl. Instrum. Methods Phys. Res., Sect. A **295**, 109 (1990).
[16] C. Cavata *et al.*, Phys. Rev. C **42**, 1760 (1990).
[17] R. Trockel *et al.*, Phys. Rev. Lett. **59**, 2844 (1987).
[18] Y. D. Kim *et al.*, Phys. Rev. Lett. **67**, 14 (1991).
[19] Y. D. Kim *et al.*, Phys. Rev. C **45**, 338 (1992).
[20] D. Fox *et al.*, Phys. Rev. C **47**, R421 (1993).
[21] E. Bauge *et al.*, Phys. Rev. Lett. **70**, 3705 (1993).
[22] T. C. Sangster *et al.*, Phys. Rev. C **47**, R2457 (1993).
[23] D. Fox *et al.*, Phys. Rev. C **50**, 2424 (1994).
[24] T. Glasmacher *et al.*, Phys. Rev. C **50**, 952 (1994).
[25] R. Bougault *et al.*, Phys. Lett. B **232**, 291 (1989).
[26] W. G. Gong *et al.*, Phys. Rev. C **43**, 1804 (1991).
[27] The values of source charge and radius chosen for the trajectory calculation are smaller than those used for the EES and McFrag model calculations since the trajectory calculation is a surface emission model without light charged particle emission between successive IMF emissions.
[28] X. Z. Zhang *et al.*, Nucl. Phys. **A461**, 641 (1987); **A461**, 668 (1987).
[29] O. Schapiro *et al.*, Nucl. Phys. **A568**, 333 (1994).